2007

X-linked idiopathic infantile nystagmus associated with a missense mutation in FRMD7

Alan Shiels
Washington University School of Medicine in St. Louis

Thomas M. Bennett
Washington University School of Medicine in St. Louis

Jessica B. Prince
Washington University School of Medicine in St. Louis

Lawrence Tychsen
Washington University School of Medicine in St. Louis

Molecular Vision 2007; 13:2233-41 <http://www.molvis.org/molvis/v13/a253/>
Received 5 November 2007 | Accepted 26 November 2007 | Published 29 November 2007

X-linked idiopathic infantile nystagmus associated with a missense mutation in *FRMD7*

Alan Shiels, Thomas M. Bennett, Jessica B. Prince, Lawrence Tychsen

Department of Ophthalmology and Visual Sciences, Washington University School of Medicine, St. Louis, MO

Purpose: Infantile nystagmus is a clinically and genetically heterogeneous eye movement disorder. Here we map and identify the genetic mutation underlying X-linked idiopathic infantile nystagmus (XL-IIN) segregating in two Caucasian-American families.

Methods: Eye movements were recorded using binocular infrared digital video-oculography. Genomic DNA was prepared from blood or buccal-cells, and linkage analysis was performed using short tandem repeat (STR) and single nucleotide polymorphism (SNP) markers. Pedigree and haplotype data were managed using Cyrillic, and LOD scores calculated using MLINK. Mutation profiling of PCR-amplified exons was performed by dye-terminator cycle-sequencing and analyzed by automated capillary electrophoresis.

Results: Video-oculography of affected males recorded conjugate, horizontal, pendular nystagmus with increasing-velocity waveforms in primary gaze converting to jerk nystagmus in eccentric gaze. Linkage analysis detected significantly positive two-point LOD scores (Z) at markers DXS8078 (Z=4.82, recombination fraction [θ]=0) and DXS1047 (Z=3.87, θ=0). Haplotyping indicated that the IIN locus mapped to the physical interval DXS8057-(11.59 Mb)-rs6528335 on Xq25-q26. Sequencing of positional-candidate genes detected a c.425T>G transversion in exon-6 of the gene for FERM domain containing-7 (*FRMD7*) that cosegregated with affected and carrier status. In addition, the same change was found to cosegregate with IIN in a genetically unrelated family but was not detected in 192 control individuals.

Conclusions: The c.425T>G change is predicted to result in the missense substitution of the phylogenetically conserved leucine at codon 142 for an arginine (p.L142R), and supports a causative role for *FRMD7* mutations in the pathogenesis of XL-IIN.

Idiopathic infantile nystagmus (IIN), also referred to as congenital nystagmus (CN), congenital "motor" nystagmus (CMN), idiopathic congenital nystagmus (ICN), or congenital idiopathic nystagmus (CIN), is a genetically heterogeneous form of developmental nystagmus that usually presents between birth and 6 months of age with an estimated annual incidence of 1/20,000 [1]. IIN is a diagnosis of "primary" or isolated nystagmus after exclusion of "secondary" nystagmus associated with patent neurological disease (e.g. glioma, cortical visual impairment), or identifiable sensory visual defects including, opacities of the cornea, lens and vitreous, foveal hypoplasia in albinism and aniridia, achromatopsia, retinal dystrophies, and optic nerve hypoplasia. Classical IIN presents as conjugate, horizontal oscillations of the eyes, in primary or eccentric gaze (i.e. uniplanar), often with a preferred head turn or tilt that is associated with a fixed "null-point" where the nystagmus intensity is dampened [2]. Other associated features are restricted to strabismus (esotropia), refractive error (astigmatism), and occasionally head nodding. Eye movement recordings reveal that classical IIN is predominantly a horizontal jerk waveform, with a "diagnostic" accelerating velocity slow phase. However, pendular and triangular waveforms may also present. Less often, IIN may exhibit predominantly vertical or torsional (elliptical) waveforms. Beyond exclusion of sensory defect nystagmus and neurological nystagmus, IIN must also be carefully differentiated from certain other forms of infantile nystagmus including, fusional maldevelopment nystagmus syndrome or latent fixation nystagmus, spamus nutans syndrome, which is characterized by asymetric or unilateral nystagmus, and periodic alternating nystagmus, which resembles IIN except that the null-point shifts position in a regular cyclic pattern [2].

All three classical types of Mendelian inheritance have been reported for IIN (Table 1); however, X-linked inheritance is likely the most common form [3]. Two loci for autosomal dominant IIN have been identified on 6p12 (NYS2) [4,5] and 7p11.2 (NYS3) [6,7] with tentative evidence from haplotype analysis for additional loci [8,9]. Indeed, a third locus for autosomal donminant nystagmus (NYS4) has been mapped to 13q31-q33 [10,11]; however NYS4 involves vestibulocerebellar dysfunction and is clinically distinct from IIN. X-linked IIN has been associated with two physically independent loci (both symbolized NYS1) that map to Xp11.4-p11.3 [8,12] and Xq26.3-q27.1 [13-18]. In addition, a locus for infantile periodic alternating nystagmus (NYS5), which often accompanies albinism, has been assigned to chromosome X [19]. Here we define an interval on Xq for IIN and identify a mutation in the gene encoding a putative cytoskeletal protein referred to as four-point-one (4.1), ezrin, radixin,

Correspondence to: A. Shiels, Department of Ophthalmology and Visual Sciences, Campus Box 8096, Washington University School of Medicine, 660 South Euclid Ave., St. Louis, MO, 63110; Phone: (314) 362-1637; FAX: (314) 362-1646; email: shiels@vision.wustl.edu

moesin (FERM) domain containing-7 (*FRMD7*), which was recently associated with XL-IIN [20-24].

METHODS

Participants and ophthalmic exams: Ethical approval for this study was obtained from the Washington University Human Research Protection Office, and written informed consent was provided by all participants prior to enrollment in accordance with the tenets of the Declaration of Helsinki. Participants were ascertained from the ophthalmic records at St. Louis Children's Hospital. Blood samples were collected by venepuncture (about 20 ml) or finger-stick (about 200 µl) into K_2EDTA vacutainer or microtainer tubes (BD Biosciences, San Jose, CA), respectively. Buccal-cell samples were self-collected into 50 ml conical tubes (Falcon; BD Biosciences) after vigorous rinsing (about 30 s) with Scope (about 20 ml) mouthwash (Procter & Gamble, Cincinnati, OH).

Ophthalmologic examination included: best-corrected visual acuity in each eye (using optotypes at 33 cm and 6 m), cycloplegic refraction, visual field testing, pupillary examination for isocoria and afferent defects, slit lamp examination with retro-illumination, ocular motor examination for strabismus (cover testing), binocular sensorial testing of fusion and stereopsis (Titmus and Randot tests), and dilated funduscopic examination of the optic nerves, maculae, and peripheral retinae. Care was taken to verify absence of signs of ocular or oculocutaneous albinism, e.g. iris transillumination defects, foveal hypoplasia and fundus hypopigmentation. Pattern visually-evoked potentials were recorded (using an array of electrodes across the occiput) to rule-out the abnormal chiasmal decussation responses characteristic of albinotic or achiasmatic retino-geniculo-striate visual pathways. Nystagmus waveforms were recorded using binocular digitial, infra-red oculography (3D VOG, SensoMotoric Instruments, Teltow, Germany) at a spatiotemporal resolution of 0.02°/60 Hz.

Genotyping and linkage analysis: Genomic DNA was extracted from peripheral blood leukocytes using the QIAamp DNA blood maxi kit (Qiagen, Valencia, CA) or from buccal-cell samples using the Puregene Mouthwash kit (Qiagen), and quantified by absorbance at 260 nm (GeneQuant *pro*; GE Healthcare, Waukesha, WI). X-chromosome short tandem repeat (STR) markers from the combined \Genethon, Marshfield, and deCODE genetic linkage maps (National Center for Biotechnology Information [NCBI]) were polymerase chain reaction (PCR) amplified with M13-tailed primers [25] in the presence of an IRDye800 labeled M13-universal primer (Li-Cor, Lincoln, NE), and detected using a 4200 DNA analyzer running Gene ImagIR software (Li-Cor) as described previously [26]. Single nucleotide polymorphism (SNP) markers from the SNP database (dbSNP, NCBI), were PCR amplified with M13-tailed primers designed from the flanking sequence (250-500 bp apart) using appropriate software (e.g. PrimerQuest, idtdna.com), and scored by sequencing essentially as described for mutation analysis below. Pedigree and haploptype data were managed using Cyrillic (v.2.1) software (FamilyGenetix Ltd., Reading, UK), and two-point LOD scores (Z) calculated using the MLINK sub-program from the LINKAGE (5.1) package of programs [27] assuming X-linked dominant inheritance with 45% penetrance in females. Marker allele frequencies were assumed to be equal, and a gene frequency of 0.0001 was assumed for the disease locus.

Mutation analysis: Genomic sequence for *FRMD7* was obtained from the Entrez human genome browser (NCBI), and gene-specific M13-tailed PCR primers were selected from the NCBI resequencing amplicon (RSA) probe database (NCBI). Genomic DNA (1 ng/µl, 10-50 µl reactions), was amplified (35-40 cycles) in a GeneAmp 9700 thermal cycler using AmpliTaq Gold Universal PCR Master Mix (Applied Biosystems, Foster City, CA) and gene-specific primers (25 pmol). Resulting PCR amplicons (about 250-500 bp) were either enzyme-purified with ExoSAP-IT (USB Corporation, Cleveland, OH) or gel-purified with the QIAquick gel-extraction kit (Qiagen). Purified amplicons were direct cycle-sequenced in both directions with BigDye Terminator Ready Reaction Mix containing M13 forward or reverse sequencing primers then ethanol precipitated and detected by capillary electrophoresis on a 3130xl Genetic Analyzer running Sequence Analysis (v 5.2) software (Applied Biosystems).

For restriction fragment length analysis, exon-6 of *FRMD7* was amplified from pedigree DNA and from the Human Random Control DNA Panels 1 and 2 (Sigma-Aldrich, St. Louis, MO) as described for sequencing above, then digested (37 °C for 1 h) with *Bsp*1286I (5 U/µl; New England BioLabs, Ipswich, MA), and visualized (302 nm) on 2% agarose/0.05% ethidium bromide gels.

Table 1. A genetic map of inherited nystagmus

Chromosome	Locus	Inheritance	Phenotype	MIM No.	Reference
6p12	NYS2	AD	Idiopathic infantile nystagmus (IIN)	164100	[4]
7p11.2	NYS3	AD, t(7;15)	IIN	608345	[6,7]
13q31-q33	NYS4	AD	Vestibulocerebellar disorder	193003	[10,11]
Xp11.4-p11.3	"NYS1"	XLD (IP)	IIN		[8,12]
Xq26.3-q27.1	NYS1	XLD (IP)	IIN	310700	[13-18,20-24]
X	NYS5	XL	Periodic alternating nystagmus (PAN)	300589	[19]

Genetic loci that have been mapped for inherited forms of developmental nystagmus. AD denotes autosomal dominant inheritance. XL denotes X-linked inheritance. XLD(IP) denotes X-linked dominant inheritance with incomplete penetrance in females. Note that autosomal recessive nystagmus (OMIM 257400) has not been mapped.

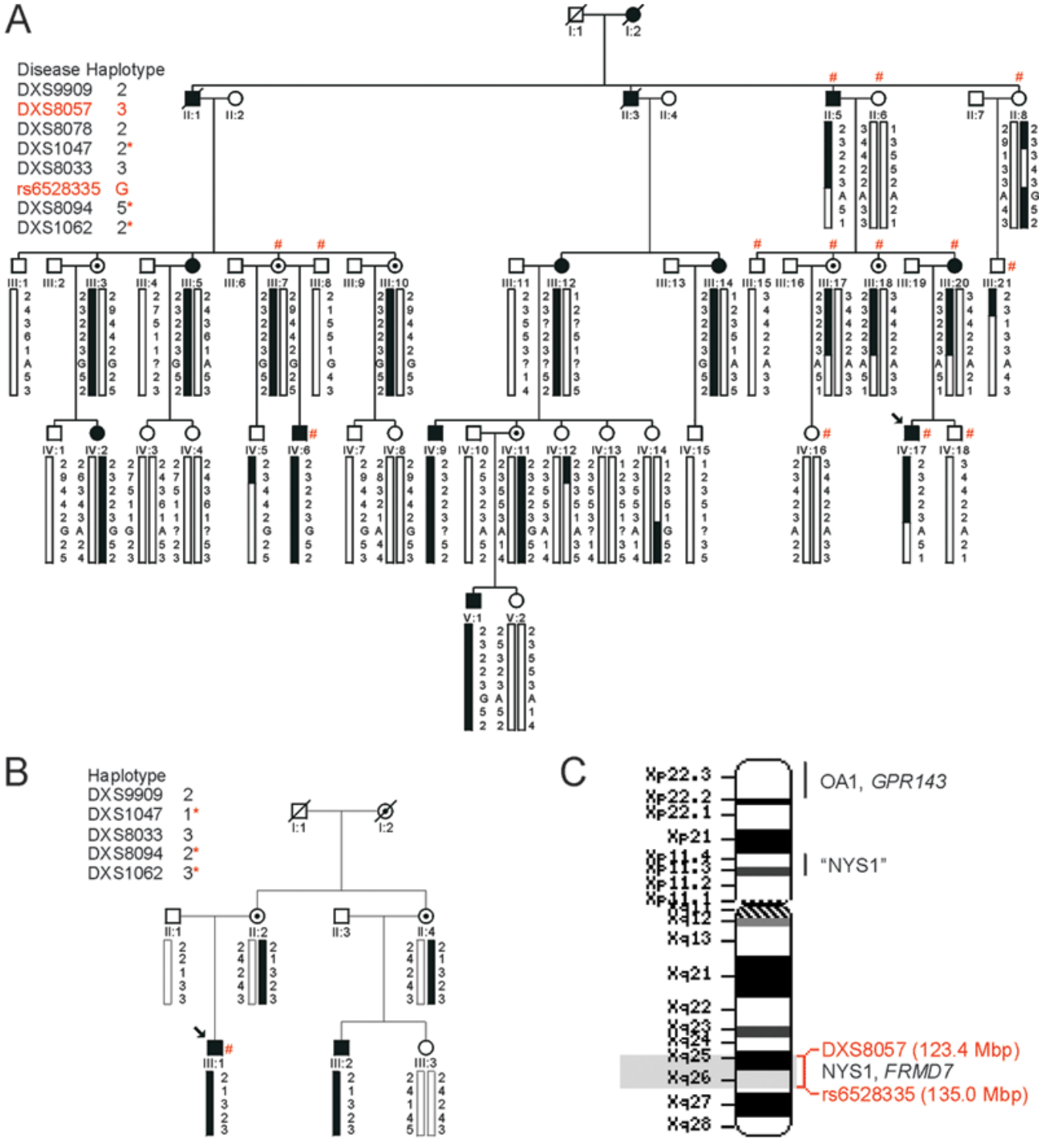

Figure 1. Familial X-linked idiopathic infantile nystagmus (IIN). **A**: Pedigree and haplotype analysis of family W showing segregation of 7 STR and 1 SNP marker on Xq, listed in descending order from the centromere. Individuals marked with a sharp (hash mark) underwent detailed ophthalmic examination. **B**: Pedigree and haplotype analysis of family M showing allelic differences with family W at markers DXS1047, DXS8094, and DXS1062. **C**: Ideogram of chromosome-X showing the cytogenetic locations of markers defining the IIN locus in this study (red) and the NYS1 (*FRMD7*) locus on Xq. The ocular albinism-1 (OA1, *GPR143*) and NYS1 loci on Xp are also indicated.

RESULTS

Pedigree structures: We studied two extended Caucasian-American families (W and M) diagnosed with IIN in the absence of detectable sensory visual defects or neurological abnormalities (Figure 1). In family W, we ascertained about 50 members spanning 5-generations (Figure 1A), including 7 affected males (2 deceased), and 6 affected females (1 deceased). X-linked inheritance was supported by the absence of father-to-son transmission and the presence of unaffected (carrier) mother-to-son transmission. Of the 9 obligate female carriers in generation-3 (daughters of affected fathers), 4 were affected (III:5, III:12, III:14, III:20) indicative of X-linked dominant inheritance with incomplete penetrance (about 45%) among females. Skewed X-inactivation is an attractive explanation for such variable penetrance; however, its role in IIN is controversial [23].

In addition, we ascertained 9 members of family M spanning 3-generations (Figure 1B) including 2 affected males (III:1, III:2). Transmission was consistent with X-linked inheritance. However, the pedigree was of insufficient size to exclude the possibility of autosomal dominant inheritance with incomplete penetrance or autosomal recessive inheritance.

Ocular phenotypes: Detailed ophthalmic examination of 14 members from family W (Figure 1) including 7 males (3 affected) and 7 females (1 affected) was undertaken by one of us (L.T.). All examined individuals in family W (age range 8-66 years) displayed clinically normal color vision, pupillary light reflexes, anterior segment, retina (including fovea), and optic nerve head. Visual acuity (best corrected with refraction) was 20/40 in both eyes of affected family members; Randot stereopsis was normal; and cycloplegic refractive errors showed moderate myopic astigmatism OU (spherical 3/4 -4.50 D; cylinder 3/4 4.00 D). Unaffected family members had moderate myopia and best corrected acuities of 20/20 OU. No iris transillumination defects were present, and the absence of ocular albinism was confirmed in one affected male (IV:17) by the presence of normal pattern visual evoked potentials (data not shown). IIN was diagnosed before 6 months of age

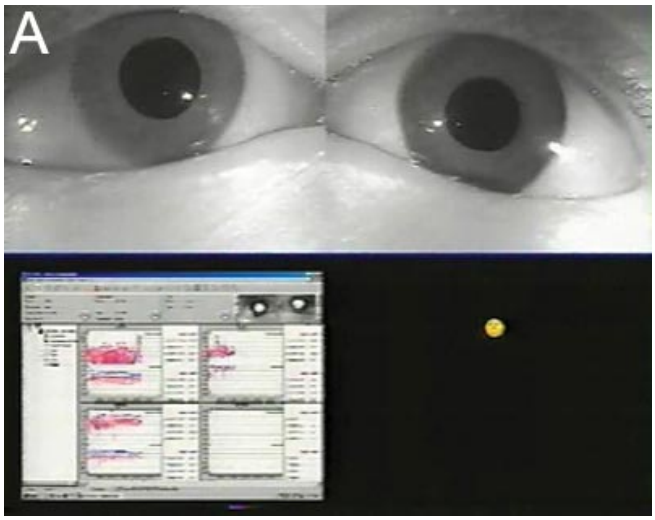

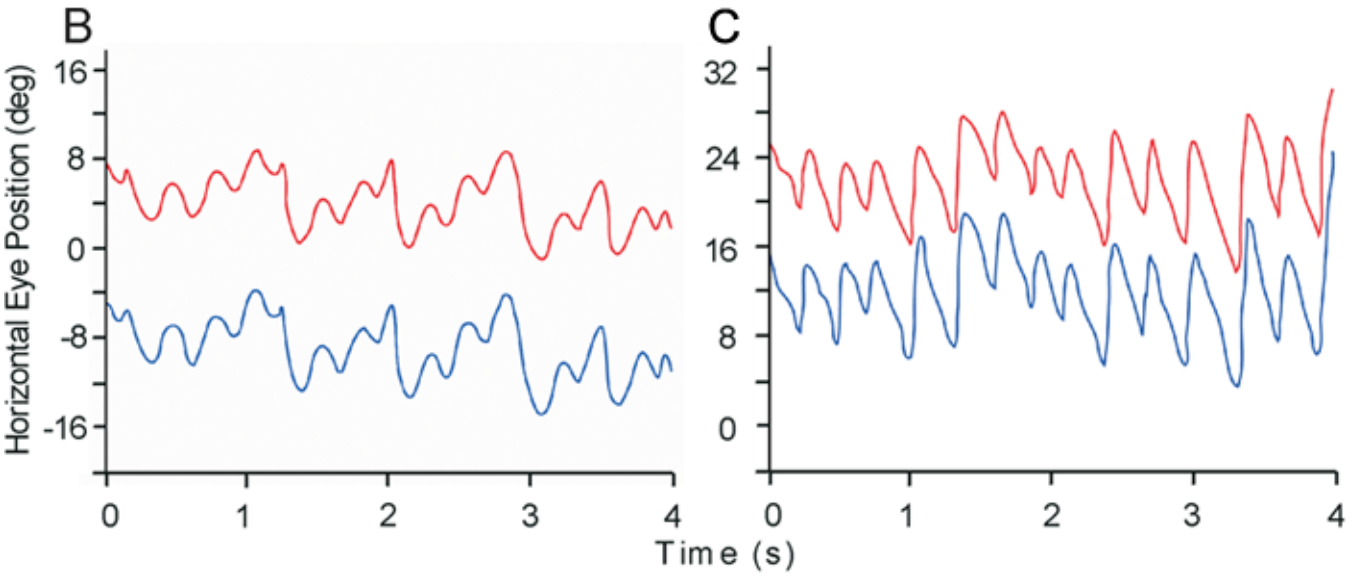

Figure 2. Nystagmus waveforms of affected male IV:6 (8 years old) in family W. **A**: Movie of eye movement recordings of affected male IV:6 (8 years of age) from family W, using binocular infrared digital video-oculography. (There is a quicktime movie of this figure in the online version of this article. A representative frame is included here). **B**: Conjugate, pendular-and-increasing-velocity waveform in right (red) and left (blue) eye when fixating stationary target at straight-ahead (primary, 0°) gaze. Note very-low-velocity rounded epochs of brief foveation during each pendular cycle. **C**: Nystagmus converts to jerk waveform in both eyes when required to fixate a target in eccentric (16° right) gaze. Note that the slide bar at the bottom of the quicktime movie can be used to manually control the flow of the movie. If you are unable to view the movie, a representative frame is included below. This animation requires Quicktime 6 or later. Quicktime is available as a free download.

in 3 males (II:5, IV:6, IV:17) and 1 female (III:20) and an abnormal head turn (left 20-50°) was evident in all four affected individuals, consistent with a null-zone. Infrared eye movement recordings were obtained from two affected males (IV:6, IV:17). Both patients were found to have conjugate, horizontal nystagmus (see movie in Figure 2A), and the oscillation was consistent with a combination of pendular and jerk waveforms (Figure 2B). Similar ophthalmic examination and testing of the male proband (III:1) in family M (Figure 1B) was consistent with a diagnosis of "non-albinotic" IIN, accompanied by a mild left head turn and occasional head oscillations.

Linkage to Xq: In order to confirm X-linked inheritance in family W, we genotyped 38 relatives (Figure 1A) including 5 affected males, 5 affected females, 6 carrier females, 17 unaffected individuals and 5 spouses with STR markers spanning the nystagmus loci previously mapped on Xp and Xq. After exclusion of the Xp locus with marker DXS8012 (Z=-1.06, θ=0.05), we obtained significant evidence of linkage (Table 2) to the Xq locus (NYS1) at markers DXS8078 (Z=4.82, θ=0.00), DXS1047 (Z=3.87, θ=0.00), and DXS8033 (Z=3.69, θ=0.00).

Haplotyping with STR and SNP markers detected 10 recombinant individuals within pedigree W (Figure 1A). First, 2 unaffected females (II:8, IV:12) and 2 unaffected males (III:21, IV:5) were recombinant proximally at DXS8057. Second, 2 affected males (II:5, IV:17), 1 affected female (III:20), 2 carrier females (III:17, III:18), and 2 unaffected females (II:8, IV:14) were obligate recombinants distally at rs6528335. However, no further recombination events were detected at intervening markers, indicating that the IIN locus lay in the physical interval, DXS8057-(11.59 Mb)-rs6528335 on Xq25-q26 (Figure 1C). Family M had insufficient meioses to provide independent evidence of linkage to the Xq interval; however, haplotype analysis indicated that family M was genetically unrelated to family W (Figure 1B).

Mutation in FRMD7*:* Our IIN interval contained about 105 positional-candidate genes (NCBI map viewer; build 36), including the 12-exon gene now symbolized *FRMD7* (GeneID: 90167; formerly LOC90167). Prior to the identification of *FRMD7* [20], we had excluded the presence of coding or splice-site mutations in 5 other candidate genes (*GPR119*, *MBNL3*, *CXX1*, *ZNF75*, *TMEM32*) with expressed sequence tags (ESTs) in eye and/or brain (data not shown). Subsequent resequencing

Table 2. Two-point LOD scores (Z) for linkage between the IIN locus in family W and markers on chromosome X

Marker	Mb	Z @ θ = 0.00	0.05	0.10	0.20	0.30	0.40	Z_{Max}	θ_{Max}
DXS8064	117.16	-∞	0.71	1.11	1.21	0.98	0.56	1.23	0.17
DXS8067	119.24	-∞	2.13	2.16	1.86	1.36	0.74	2.17	0.08
DXS1001	119.72	-∞	2.41	2.40	2.04	1.49	0.80	2.43	0.07
DXS1212	122.31	-∞	0.53	0.71	0.72	0.56	0.31	0.75	0.15
DXS9909	122.36	1.60	1.48	1.35	1.07	0.75	0.39	1.60	0.00
DXS8057	123.40	-∞	1.80	1.90	1.69	1.26	0.69	1.90	0.10
DXS8009	126.00	3.29	3.03	2.75	2.14	1.46	0.73	3.29	0.00
DXS8078	126.37	4.82	4.41	3.99	3.07	2.06	1.00	4.82	0.00
DXS1047	128.90	3.87	3.55	3.21	2.49	1.70	0.86	3.87	0.00
FRMD7 c.425T>G	131.04	4.99	4.59	4.16	3.25	2.24	1.14	4.99	0.00
DXS8033	133.92	3.69	3.41	3.10	2.45	1.72	0.91	3.69	0.00
rs6528335	134.99	-2.75	-0.44	-0.21	-0.04	0.02	0.02	0.02	0.37
DXS8094	136.06	3.33	3.06	2.77	2.16	1.51	0.79	3.33	0.00
DXS1041	136.36	1.72	1.56	1.40	1.07	0.71	0.35	1.72	0.00
DXS8050	136.81	2.43	2.22	2.01	1.56	1.07	0.55	2.43	0.00
DXS1062	137.13	0.52	2.31	2.34	2.04	1.52	0.85	2.35	0.08
DXS1211	138.13	0.27	2.06	2.08	1.77	1.27	0.67	2.10	0.08

Z values for markers on Xq listed in physical order, measured in megabases (Mb), from the short-arm telomere (Xp-tel). The maximum Z values (Zmax) occurred at marker DXS8078, and at the c.425T>G transversion in exon-6 of *FRMD7*. θ=recombination fraction.

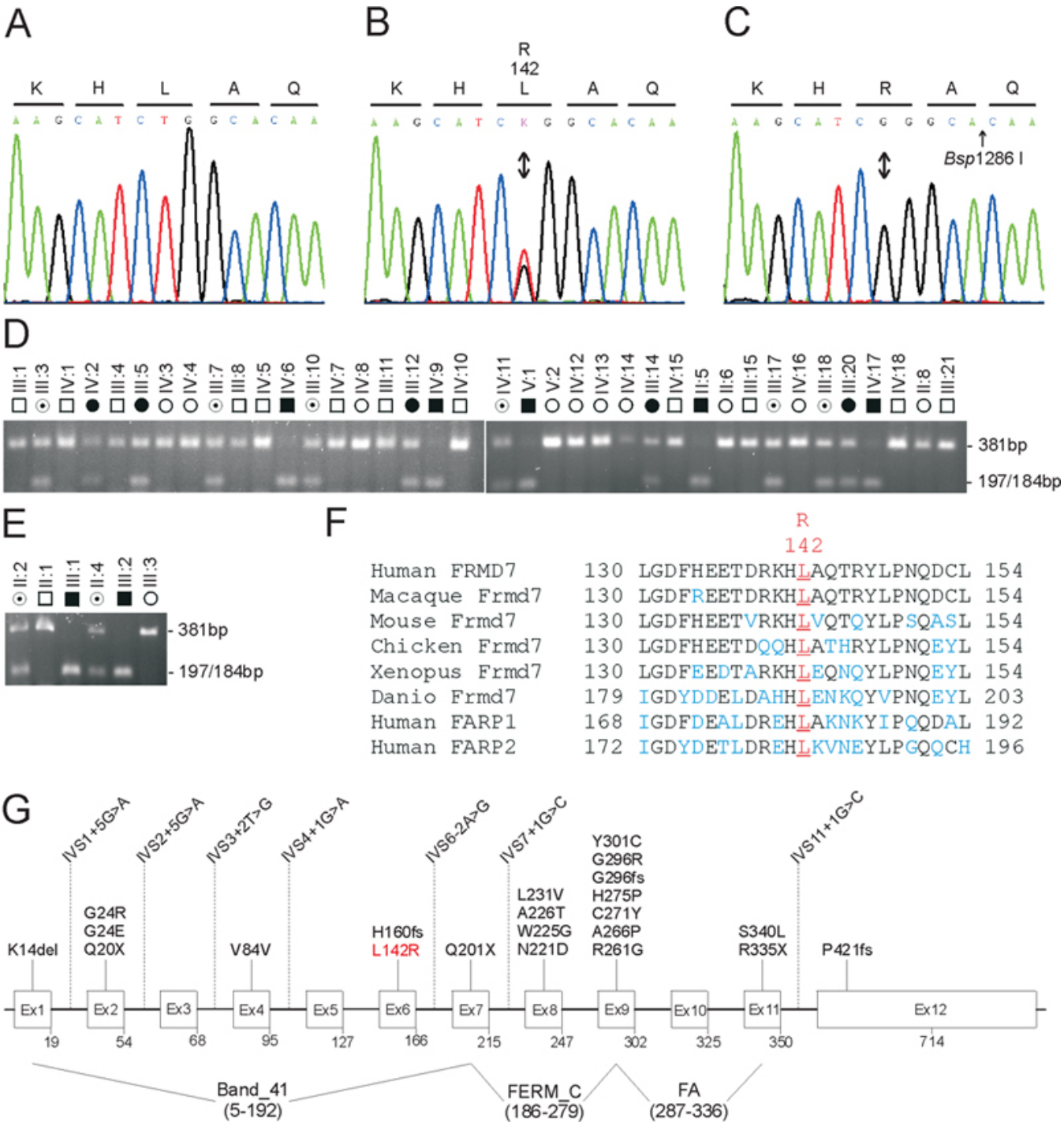

Figure 3. Mutation analysis of *FRMD7*. **A**: Sequence trace of the wild type allele, showing translation of leucine (L) at codon 142 (CTG). **B**: Sequence trace of the heterozygous mutant allele, showing the c.425T>G transversion (denoted as K by the International Union of Pure and Applied Chemistry [IUPAC] code) that is predicted to result in the missense substitution of arginine (R) for leucine at codon 142 (p.L142R). **C**: Sequence trace of the hemizygous mutant allele showing translation of arginine (R) at codon 142 (CGG). **D**-**E**: Restriction-fragment-length analysis showing gain of a *Bsp*1286I site (5'-GGGCA/C) that cosegregates only with affected and carrier individuals hemizygous or heterozygous for the c.425T>G transversion (197/184 bp) in family W (**D**) and family M (**E**). **F**: Amino acid sequence alignment of human FRMD7 and orthologs from other species, showing phylogenetic conservation of p.L142. **G**: Exon organization and mutation profile of *FRMD7*. Codons are numbered below each exon. So far, more than 30 mutations have been reported [20-24]. Note the synonymous p.V84V polymorphism (c.252G>A) creates a cryptic splice acceptor-site in exon 4 resulting in missplicing [20].

of *FRMD7* in family W detected a hemizygous c.425T>G transversion in exon-6 of *FRMD7* (Figure 3) in two affected males (II:5, IV:6) that was not present in an unaffected male (III:1). The same heterozygous change was also present in an affected female (III:14). Surprisingly, in family M we identified the same hemizygous and heterozygous change in the affected proband (III:1) and his carrier mother (II:4), respectively. In addition, we detected normal allelic variations at 6 SNPs spanning *FRMD7* (Table 3) that were not present in family W, confirming that the families were genetically unrelated.

The c.425T>G transversion introduced an adjacent *Bsp*1286 I restriction-enzyme site and allele-specific restriction-fragment-length analysis confirmed that the G-allele cosegregated with affected and carrier individuals in both families W and M, but was not present in unaffected relatives (Figure 3D,E). Furthermore, when we tested the c.425T>G transversion as a biallelic marker in Family W, with a notional allelic frequency of 1%, in a two-point LOD score analysis of the IIN locus (Table 2) we obtained further compelling evidence of linkage (Z=4.99, θ=0). In addition, we confirmed that the c.425T>G transversion was not listed in dbSNP (NCBI), and excluded it as a SNP in a panel of 192 normal unrelated individuals (288 X-chromosomes) using *Bsp*1286 I restriction analysis (data not shown). While it is possible that an undetected mutation lay elsewhere within the disease-haplotype interval, our genotype data in families W and M strongly suggested that the c.425T>G transversion in exon-6 of *FRMD7* represented a causative mutation rather than a benign SNP in linkage disequilibrium with the XL-IIN phenotype.

The c.425T>G transversion occurred at the second base of codon 142 (CTG>CGG), and was predicted to result in a leucine-to-arginine missense substitution (p.L142R) at the level of protein translation. Cross-species alignment of FRMD7 amino-acid sequences in the Entrez protein database using ClustalW revealed that p.L142 is phylogenetically conserved from zebrafish to man (Figure 3F). Moreover, the predicted p.L142R substitution reflected a non-conservative amino acid change, with the neutral hydrophobic side-group of leucine replaced by the basic side-group of arginine. Position-specific score matrix analysis, using the PSSM, showed a decline in score from +4 to -2 (Table 4) confirming that the predicted p.L142R substitution occurred less frequently than expected in proteins with the conserved FERM domain (Conserved Domain Database, pfam00373), further raising the likelihood of functional consequences.

Table 3. *FRMD7* sequence variations detected in family M

SNP	Location	Alleles*	Codon
rs5933084	5′-Upstream	G/C	
rs5930546	Exon 2	C/T	S23S
rs5933067	IVS4 (-104)	G/C	
rs5977623	Exon 12	T/C	I511I
rs3764771	3′-UTR	A/T	
rs41312755	3′-UTR	G/A	

Single nucleotide polymorphisms (SNPs) detected during resequencing of the *FRMD7* gene in family M. All 6 SNPs were found in the heterozygous state. The asterisk indicates that the reference allele is shown on the left. The SNPs in exon 2 and exon 12 resulted in synonymous amino acid changes at serine 23 and isoleucine 511, respectively. IVS denotes intervening (intron) sequence. UTR denotes untranslated region.

DISCUSSION

In this study, we have mapped an interval for XL-IIN (DXS8057-[about 11.6 Mb]-rs6528335) to the NYS1 locus on Xq25-q26, and identified a missense mutation in *FRMD7* (c.425T>G, p.L142R). Our disease interval overlaps that described recently (DXS1047-[about 7.5 Mb]-DXS1041) [20], and when combined these data refine the NYS1 locus to DXS1047-(about 6.1 Mb)-rs6528335. The p.L142R mutation was detected in two genetically unrelated Caucasian-American families, and has also has been described in a family of Irish ancestry [20], providing further evidence for *FRMD7* mutations in the pathogenesis of XL-IIN.

FRMD7 encodes a 714 amino acid protein belonging to the FERM domain super-family of proteins, which mediate linkage of plasma-membrane proteins to the cortical-cytoskeleton [28]. Interestingly, FRMD7 is evolutionarily related to the FERM, Rho guanine-nucleotide exchange factor, plekstrin homology domain proteins, FARP1 and FARP2, with all three proteins sharing about 50% identity within the FERM domain. So far, most of the mutations reported in *FRMD7* reside in

Table 4. Position specific score matrix (PSSM) analysis of the predicted p.L142R substitution in FRMD7

Codon	Amino acid	Side chain	Charge	Potential H-bonds	Mol. Wt.	Isoelectric point	Hydrophobicity	PSSM value
CTG	L (Leu)	$-CH_2-CH-C_2H_6$	0	0	113	6.0	0.918	4
CGG	R (Arg)	$-C_3H_6-NH-C-N_2H_4$	+	7	156	10.8	0.000	-2

Differences in the physico-chemical properties of leucine (L) and arginine (R) are consistent with a nonconservative substitution. The negative PSSM value indicates that arginine substitutes for leucine at position 142 less frequently than expected among proteins containing the conserved FERM domain.

exons 1-11 (Figure 3G), which encode the FERM-domain and the FERM-adjacent domain [20-22]. The FERM-domain is a protease-resistant region comprising 200-300 amino acids (about 30 kDa), arranged in a globular 3-lobed or cloverleaf-like structure usually located near the NH_2-terminus, which binds a variety of membrane protein and lipid ligands [29]. Similarly, the FERM-adjacent (FA) domain is a protease-resistant region of about 60 amino acids (about 16 kDa), juxtaposed on the COOH-terminal side of the FERM domain, and is believed to act as a regulator of the latter's protein/lipid binding activity [30].

FRMD7 is expressed in most adult human tissues, and has been detected in the developing neuroretina and regions of the embryonic brain known to control eye movement [20]; however, its precise function remains unknown. Interestingly, FARP1 has been implicated in the regulation of microfilament organization [31], and FARP2 has been shown to be involved in neurite re-modeling and axonal repulsion [32,33], suggesting that FRMD7 may also perform a dynamic neurocytoskeletal function. In addition to enhanced diagnostic testing and genetic counseling for IIN in a clinical setting, continued studies of *FRMD7* will provide new insights regarding the molecular control of eye movement and the development of binocular vision.

ACKNOWLEDGEMENTS

We thank family members for participating in this study, and Jennifer King for assistance with DNA preparation. This work was supported by NIH/NEI grants EY012284 (A.S.), EY10214 (L.T.), and EY02687.

REFERENCES

1. Casteels I, Harris CM, Shawkat F, Taylor D. Nystagmus in infancy. Br J Ophthalmol 1992; 76:434-7.
2. Reinecke RD. Costenbader Lecture. Idiopathic infantile nystagmus: diagnosis and treatment. J AAPOS 1997; 1:67-82.
3. Self J, Lotery A. The molecular genetics of congenital idiopathic nystagmus. Semin Ophthalmol 2006; 21:87-90.
4. Kerrison JB, Arnould VJ, Barmada MM, Koenekoop RK, Schmeckpeper BJ, Maumenee IH. A gene for autosomal dominant congenital nystagmus localizes to 6p12. Genomics 1996; 33:523-6.
5. Kerrison JB, Koenekoop RK, Arnould VJ, Zee D, Maumenee IH. Clinical features of autosomal dominant congenital nystagmus linked to chromosome 6p12. Am J Ophthalmol 1998; 125:64-70.
6. Patton MA, Jeffery S, Lee N, Hogg C. Congenital nystagmus cosegregating with a balanced 7;15 translocation. J Med Genet 1993; 30:526-8.
7. Klein C, Vieregge P, Heide W, Kemper B, Hagedorn-Greiwe M, Hagenah J, Vollmer C, Breakefield XO, Kompf D, Ozelius L. Exclusion of chromosome regions 6p12 and 15q11, but not chromosome region 7p11, in a German family with autosomal dominant congenital nystagmus. Genomics 1998; 54:176-7.
8. Oetting WS, Armstrong CM, Holleschau AM, DeWan AT, Summers GC. Evidence for genetic heterogeneity in families with congenital motor nystagmus (CN). Ophthalmic Genet 2000; 21:227-33.
9. Hoffmann S, Becker A, Hoerle S, Metz A, Oertel WH, Sommer N, Hemmer B. Autosomal dominant congenital nystagmus is not linked to 6p12, 7p11, and 15q11 in a German family. Am J Ophthalmol 2004; 138:439-43.
10. Ragge NK, Hartley C, Dearlove AM, Walker J, Russell-Eggitt I, Harris CM. Familial vestibulocerebellar disorder maps to chromosome 13q31-q33: a new nystagmus locus. J Med Genet 2003; 40:37-41.
11. Harris CM, Walker J, Shawkat F, Wilson J, Russell-Eggitt I. Eye movements in a familial vestibulocerebellar disorder. Neuropediatrics 1993; 24:117-22.
12. Cabot A, Rozet JM, Gerber S, Perrault I, Ducroq D, Smahi A, Souied E, Munnich A, Kaplan J. A gene for X-linked idiopathic congenital nystagmus (NYS1) maps to chromosome Xp11.4-p11.3. Am J Hum Genet 1999; 64:1141-6.
13. Kerrison JB, Vagefi MR, Barmada MM, Maumenee IH. Congenital motor nystagmus linked to Xq26-q27. Am J Hum Genet 1999; 64:600-7.
14. Kerrison JB, Giorda R, Lenart TD, Drack AV, Maumenee IH. Clinical and genetic analysis of a family with X-linked congenital nystagmus (NYS1). Ophthalmic Genet 2001; 22:241-8.
15. Mellott ML, Brown J Jr, Fingert JH, Taylor CM, Keech RV, Sheffield VC, Stone EM. Clinical characterization and linkage analysis of a family with congenital X-linked nystagmus and deuteranomaly. Arch Ophthalmol 1999; 117:1630-3.
16. Zhang B, Xia K, Ding M, Liang D, Liu Z, Pan Q, Hu Z, Wu LQ, Cai F, Xia J. Confirmation and refinement of a genetic locus of congenital motor nystagmus in Xq26.3-q27.1 in a Chinese family. Hum Genet 2005; 116:128-31.
17. Guo X, Li S, Jia X, Xiao X, Wang P, Zhang Q. Linkage analysis of two families with X-linked recessive congenital motor nystagmus. J Hum Genet 2006; 51:76-80.
18. Self JE, Ennis S, Collins A, Shawkat F, Harris CM, Mackey DA, Hodgkins PR, Temple IK, Chen X, Lotery AJ. Fine mapping of the X-linked recessive congenital idiopathic nystagmus locus at Xq24-q26.3. Mol Vis 2006; 12:1211-6.
19. Hertle RW, Yang D, Kelly K, Hill VM, Atkin J, Seward A. X-linked infantile periodic alternating nystagmus. Ophthalmic Genet 2005; 26:77-84.
20. Tarpey P, Thomas S, Sarvananthan N, Mallya U, Lisgo S, Talbot CJ, Roberts EO, Awan M, Surendran M, McLean RJ, Reinecke RD, Langmann A, Lindner S, Koch M, Jain S, Woodruff G, Gale RP, Degg C, Droutsas K, Asproudis I, Zubcov AA, Pieh C, Veal CD, Machado RD, Backhouse OC, Baumber L, Constantinescu CS, Brodsky MC, Hunter DG, Hertle RW, Read RJ, Edkins S, O'Meara S, Parker A, Stevens C, Teague J, Wooster R, Futreal PA, Trembath RC, Stratton MR, Raymond FL, Gottlob I. Mutations in FRMD7, a newly identified member of the FERM family, cause X-linked idiopathic congenital nystagmus. Nat Genet 2006; 38:1242-4.
21. Schorderet DF, Tiab L, Gaillard MC, Lorenz B, Klainguti G, Kerrison JB, Traboulsi EI, Munier FL. Novel mutations in FRMD7 in X-linked congenital nystagmus. Mutation in brief #963. Online. Hum Mutat 2007; 28:525.
22. Zhang Q, Xiao X, Li S, Guo X. FRMD7 mutations in Chinese families with X-linked congenital motor nystagmus. Mol Vis 2007; 13:1375-8.
23. Self JE, Shawkat F, Malpas CT, Thomas NS, Harris CM, Hodgkins PR, Chen X, Trump D, Lotery AJ. Allelic variation of the FRMD7 gene in congenital idiopathic nystagmus. Arch Ophthalmol 2007; 125:1255-63.
24. Zhang B, Liu Z, Zhao G, Xie X, Yin X, Hu Z, Xu S, Li Q, Song F, Tian J, Luo W, Ding M, Yin J, Xia K, Xia J. Novel mutations of the FRMD7 gene in X-linked congenital motor nystagmus. Mol Vis 2007; 13:1674-9.

25. Oetting WS, Lee HK, Flanders DJ, Wiesner GL, Sellers TA, King RA. Linkage analysis with multiplexed short tandem repeat polymorphisms using infrared fluorescence and M13 tailed primers. Genomics 1995; 30:450-8.
26. Mackay DS, Andley UP, Shiels A. Cell death triggered by a novel mutation in the alphaA-crystallin gene underlies autosomal dominant cataract linked to chromosome 21q. Eur J Hum Genet 2003; 11:784-93.
27. Lathrop GM, Lalouel JM, Julier C, Ott J. Strategies for multilocus linkage analysis in humans. Proc Natl Acad Sci U S A 1984; 81:3443-6.
28. Chishtia AH, Kim AC, Marfatia SM, Lutchman M, Hanspal M, Jindal H, Liu S-C, Low PS, Rouleau GA, Mohandas N, Chasis JA, Conboy JG, Gascard P, Takakuwa Y, Huang S-C, Benz Jr EJ, Bretscher A, Fehon RG, Gusella JF, Ramesh V, Solomon F, Marchesi VT, Tsukita S, Tsukita S, Arpin M, Louvard D, Tonks NK, Anderson JM, Fanning AS, Bryant PJ, Woods DF, Hoover KB. The FERM domain: a unique module involved in the linkage of cytoplasmic proteins to the membrane. Trends Biochem Sci 1998; 23:281-2.
29. Bretscher A, Edwards K, Fehon RG. ERM proteins and merlin: integrators at the cell cortex. Nat Rev Mol Cell Biol 2002; 3:586-99.
30. Baines AJ. A FERM-adjacent (FA) region defines a subset of the 4.1 superfamily and is a potential regulator of FERM domain function. BMC Genomics 2006; 7:85.
31. Koyano Y, Kawamoto T, Shen M, Yan W, Noshiro M, Fujii K, Kato Y. Molecular cloning and characterization of CDEP, a novel human protein containing the ezrin-like domain of the band 4.1 superfamily and the Dbl homology domain of Rho guanine nucleotide exchange factors. Biochem Biophys Res Commun 1997; 241:369-75.
32. Kubo T, Yamashita T, Yamaguchi A, Sumimoto H, Hosokawa K, Tohyama M. A novel FERM domain including guanine nucleotide exchange factor is involved in Rac signaling and regulates neurite remodeling. J Neurosci 2002; 22:8504-13.
33. Toyofuku T, Yoshida J, Sugimoto T, Zhang H, Kumanogoh A, Hori M, Kikutani H. FARP2 triggers signals for Sema3A-mediated axonal repulsion. Nat Neurosci 2005; 8:1712-9.

The print version of this article was created on 29 Nov 2007. This reflects all typographical corrections and errata to the article through that date. Details of any changes may be found in the online version of the article.